

The effects of landforms and climate on NDVI in Artvin, Turkey

Hilal Turgut & Bülent Turgut

Keywords: NDVI, GIS, drought, regression, interpolation

Abstract

Artvin, located in the Caucasus ecological region, is a unique area due to its high mountains, climatic characteristics, terrestrial and aquatic ecosystems, and high biodiversity. Thus, it is a suitable area for examining the effects of landforms and climate on vegetation dynamics. Vegetation changes over a three-year period (2018 to 2020) were investigated by examining the trends in the Normalized Difference Vegetation Index (NDVI) across the study area. First, the relationships between mean temperature, total precipitation and landforms (elevation, slope, aspect and distance from the sea) were determined by regression analysis, and their interpolated maps were created. In the second stage, the effects of the same landform characteristics and climatic factors, such as total precipitation and mean temperature, on NDVI were analysed. Regression analysis showed that the relationships between precipitation and distance from the sea, and between temperature and elevation were statistically significant. They were therefore used for prediction modelling. Changes in temperature and precipitation affected the NDVI values, but precipitation was found to be more significant than temperature. Landform differences were also responsible for changes in the NDVI values; distance from the sea was the most significant factor. The study also shows that in the drier period (2018), the elevation range where NDVI decreases is lower than during the other periods (2018 and 2020). We therefore conclude that the alpine zone can be more affected during drought periods.

Profile

Protected areas

Kackar Mountain

National Park (NP), Ha-

tila Valley NP, Karagöl

Sahara NP, Camili

Biosphere Reserve,

8 regional protection

areas

Mountain range

Artvin mountain, Turkey

Introduction

Sustainable landscape management requires knowledge of abiotic ecosystem components, such as climate and topography, and needs to be able to analyse the interactions between them. Correlations between non-living environmental components (such as landforms and climate) and vegetation constitute an important basis for the creation of sustainable management strategies in today's world, where the effects of climate change are evident.

Temperature and precipitation are key climatic factors that alter the Normalized Difference Vegetation Index (NDVI) (Sanz et al. 2021), which is an indicator of the development of vegetation in terrestrial ecosystems (Myneni & Williams 1994; Xu et al. 2017; Chu et al. 2019). Like all organisms, plants need an optimum temperature range for maximum growth (Kimmins 2004). If the temperature exceeds this optimum range, it adversely affects plant growth due to decreased photosynthetic activity, and water and nutrient availability. Total annual precipitation and its distribution over the vegetation period are the main controls on vegetation structure, composition and distribution. Thus, precipitation greatly impacts the amount of vegetation (Zhang et al. 2013). Researchers have reported that drought due to climate change negatively alters vegetation growth (Gao et al. 2014; Pang et al. 2017; Nanzad et al. 2019; Li et al. 2021; Zhe & Zhang 2021), and that there is a close correlation between vegetation cover

changes and climate factors, such as temperature and rainfall (Hou et al. 2015; Liu et al. 2018).

Landforms such as elevation, aspect and slope correlate significantly with vegetation and soil patterns at meso- and microscales (El-Keblawy et al. 2015; Flores et al. 2019). This is because landform controls the intensity of the key factors important to plants and to the soils that develop with them (Jiang et al. 2021; Peilin et al. 2020; Li et al. 2020; Liu et al. 2019). Erosion, for example, restricts plant growth by decreasing soil depth and water efficiency in sloping terrain. Landforms can also affect the large-scale spatial distribution and patterns of vegetation by creating microclimates (Panigrahi et al. 2021).

The NDVI is defined as a measure of surface reflectance; it provides a quantitative estimation of vegetation growth and biomass (Wu et al. 2016). This index varies between -1 and $+1$, in which values of less than zero during the growing season indicate no vegetation cover (e.g. in areas of desert or bare earth), while values greater than zero in the growing season describe vegetation cover (Choubin et al. 2019). The NDVI value is associated with the intensity of photosynthetic activity in the vegetation observed (Piao et al. 2006; Wu et al. 2015). NDVI can accurately reflect the metabolic intensity and annual variation of vitality in vegetation; it indicates vegetation growth, and changes in temperature, precipitation and other climatic factors in the absence of human activities and natural disasters (Ghebregabher et al. 2020; Jiang et al. 2021; Liu

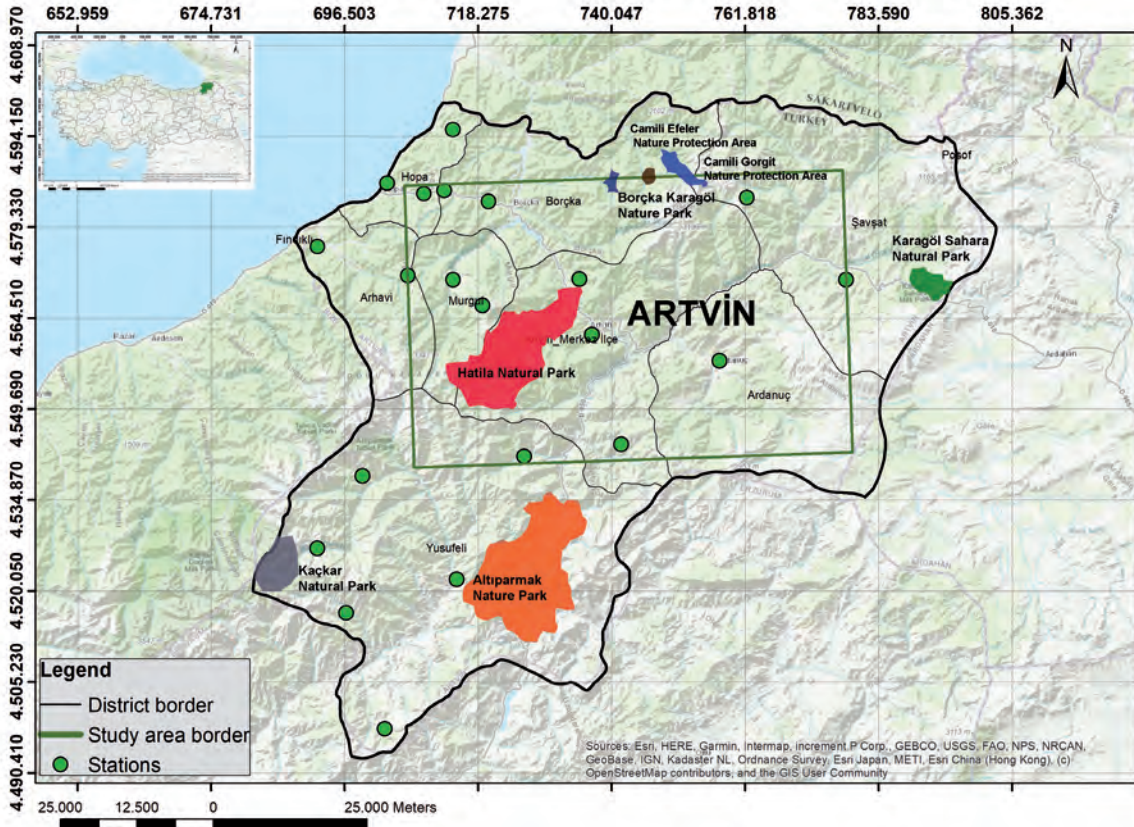


Figure 1 – Location of the study area and of the meteorological observation stations.

et al. 2019; Poll et al. 2009). Thus, NDVI has been widely used to monitor vegetation dynamics and determine the effect of climate variations such as cooling and warming on vegetation in the global (Nemani et al. 2003; Zhu et al. 2016) and regional (Piao et al. 2006; Wu et al. 2015) scale.

Its particular geographical location and topography make Artvin both a special region for climatic variation, and Turkey's richest region in terms of biodiversity (Eminağaoğlu et al. 2015). Within the borders of Artvin, there are three National Parks (NP) (Kaçkar Mountains NP, Hatila Valley NP, Karagöl-Sahara NP), three Nature Protection Areas (NPA) (Camili-Efeler NPA, Camili-Gorgit NPA, Çamburnu NPA), five Natural Parks (NaP) (Altıparmak Mountains NaP, Balıklı-Güneşli Waterfalls NaP, Borçka-Karagöl NaP, Cehennem Deresi Canyon NaP, Tavşan Hill NaP), and Camilli Biosphere Reserve. Due to the variability in topography, climate and vegetation, even over short distances, Artvin is a suitable study area for observing the effects of climatic and topographical factors on the temporal and spatial variability of vegetation. Nowadays, the effects of climate change on ecosystems are observed across the globe. For this reason, new tools and methods are necessary to understand ecosystem components and predict possible changes. By using NDVI, the effects of changes in the abiotic environment on the ecosystem can be determined. The aim of this study was to identify the effects of climatic parameters (such as precipitation and temper-

ature), and landforms (such as elevation, aspect, slope and distance from the sea) on the NDVI during the three years 2018, 2019 and 2020. The results of this study will be useful for practitioners in estimating the possible consequences of climate change and managing sites accordingly.

Materials and Methods

Study area

The study area located in Artvin province is bounded by 455230527235 N and 4585102-4539220 E according to UTM WGS 1984 coordinate system (Figure 1). Topographically, it is defined by deep

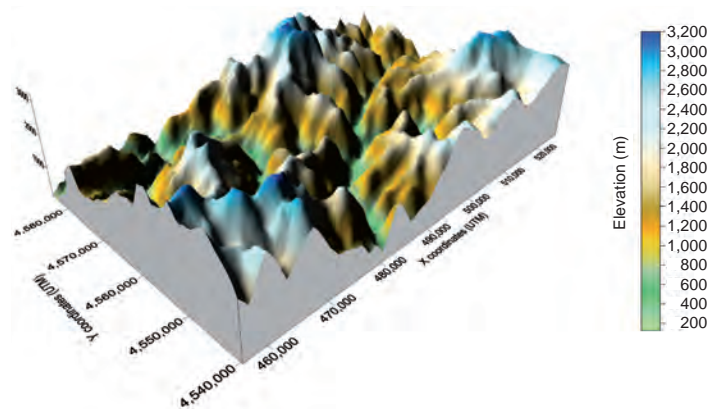


Figure 2 – The surface of the study area in 3D.

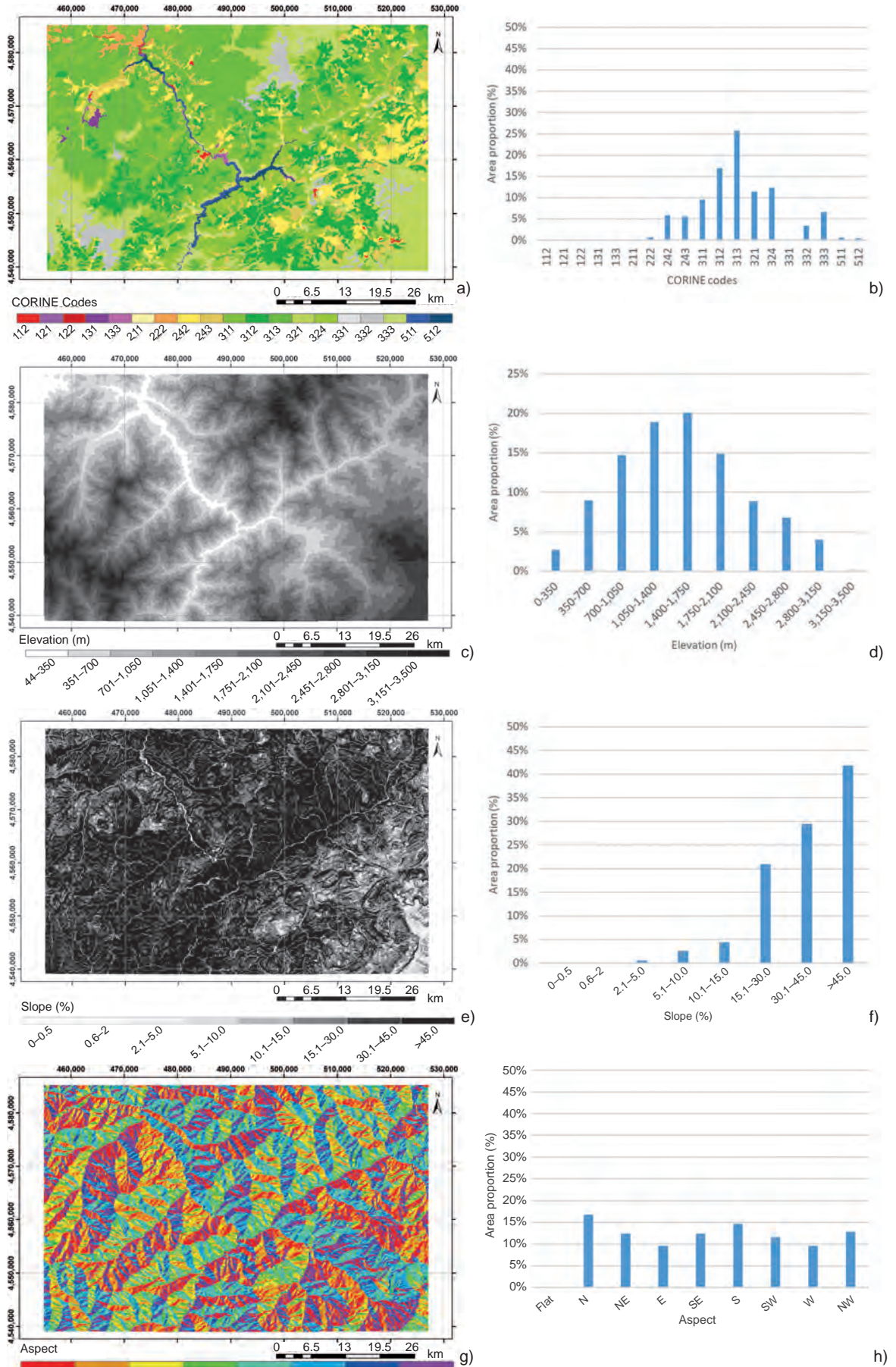


Figure 3 – (a) Corine land use map and (b) the area proportion of the Corine classes; (c) elevation map of the study area and (d) the area proportion of the elevation classes; (e) slope map of the study area and (f) area proportion of the slope classes; (g) aspect map of the study area and (h) area proportion of the aspects.

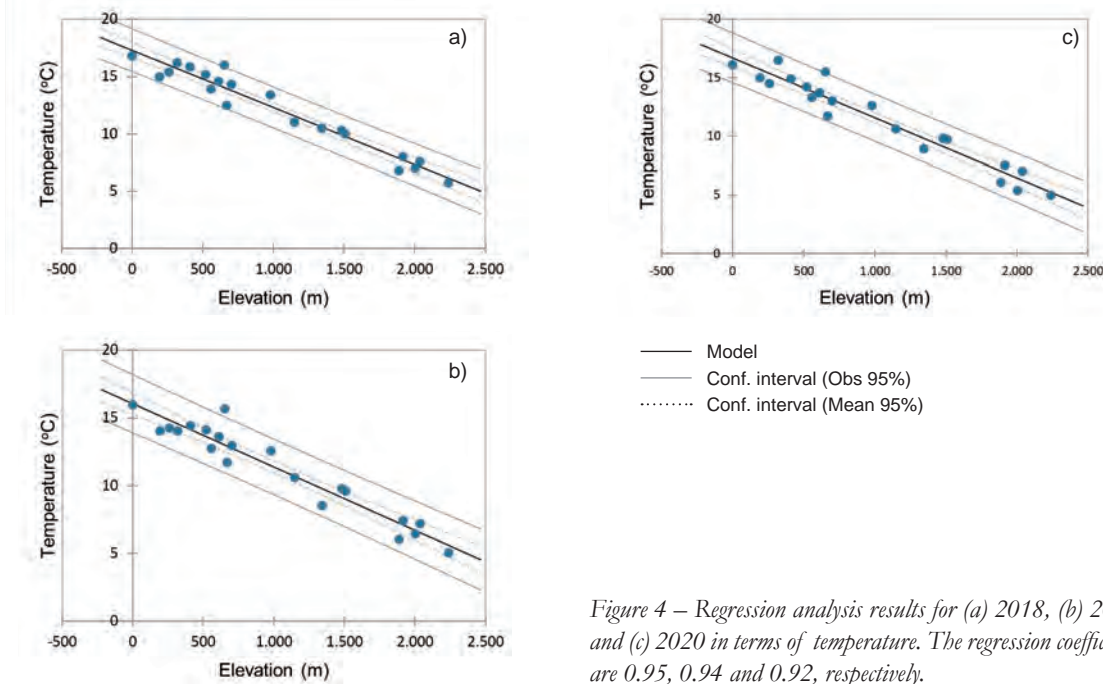


Figure 4 – Regression analysis results for (a) 2018, (b) 2019, and (c) 2020 in terms of temperature. The regression coefficients are 0.95, 0.94 and 0.92, respectively.

valleys and high mountains, so there are considerable variations in elevation and slope, even over short distances (Figure 2). There are four dams in the study area (the Muratlı, Borçka, Deriner and Artvin Dams), built on the Çoruh River to generate hydroelectric power. According to the CORINE land-cover classes, the area comprises 19 different land-use cases (Figure 3a), and forest and seminatural areas cover 86% of study area (Figure 3b). In terms of its flora, Artvin is the richest province in Turkey, with a total of 2,727 plant taxa belonging to 137 families and 761 genera (Eminağaoğlu et al. 2015). According to the Thornthwaite climate classification system, the study area includes six classes: wet (A), humid (B1, B2, B3, B4), and semi-humid (C2) (Turkish State Meteorological Services 2021; <https://www.mgm.gov.tr/iklim/iklim-siniflandirmalari.aspx>).

The elevation is the lowest in the Coruh riverbed, but reaches 3,400 m in the mountains (Figure 3c). We divided the elevation range into 350 m bands. The range 1,400–1,750 m, accounting for 20.1% of the study area, is the single most extensive altitude class. The least extensive is 3,150–3,500 m (Figure 3d). Steep terrain is common (Figure 3e): in 42% of the study area, the slope is >45% (Figure 3f). Since the mountains in the area extend east-west, the predominant aspects are north- and south-facing (Figure 3g), with north-facing being the most common (16.82%) (Figure 3h).

Data and analysis methods

Mapping landforms

A digital elevation model, slope, distance from the sea and aspect were computed for the study area using the *Spatial analyst* tool in ArcGIS software and Alos Palsar satellite imagery with a resolution of 12.5 m (ASF DAAC 2015). Due to the large size of the study area, maps were created by combining images taken on various cloudless days in 2019, using ArcGIS *image analysis* tools. The slope map created used the classification system recommended by the FAO (2021).

Obtaining climate data and creating interpolated maps

The results of the statistical analyses showed that the years 2018, 2019 and 2020 had significant differences in terms of temperature and precipitation. For this reason, data from these three years were evaluated in the study. The choice of consecutive years minimizes the effects of other factors, such as anthropogenic ones, which may have an impact on NDVI. Meteorological data for 2018, 2019 and 2020, including annual total precipitation and annual mean temperature, were collected from 22 meteorological observation stations of the Turkish State Meteorological Service in Artvin (Figure 1). Their geographical coordinates and elevation were obtained, and their distances from the sea were determined using the ArcGIS software. The fol-

Table 1 – Prediction models determined using regression analysis.

Years	Temperature	Precipitation
2018	$17.29 - (0.00499 * \text{Elevation})$	$[0.0000005 * (\text{Distance to sea})^2] - (0.0589 * \text{Distance from sea}) + 2,202.4$
2019	$16.70 - (0.00512 * \text{Elevation})$	$[0.0000006 * (\text{Distance to sea})^2] - (0.0676 * \text{Distance from sea}) + 2,148.1$
2020	$16.04 - (0.00467 * \text{Elevation})$	$[0.0000006 * (\text{Distance to sea})^2] - (0.0677 * \text{Distance from sea}) + 2,450.5$

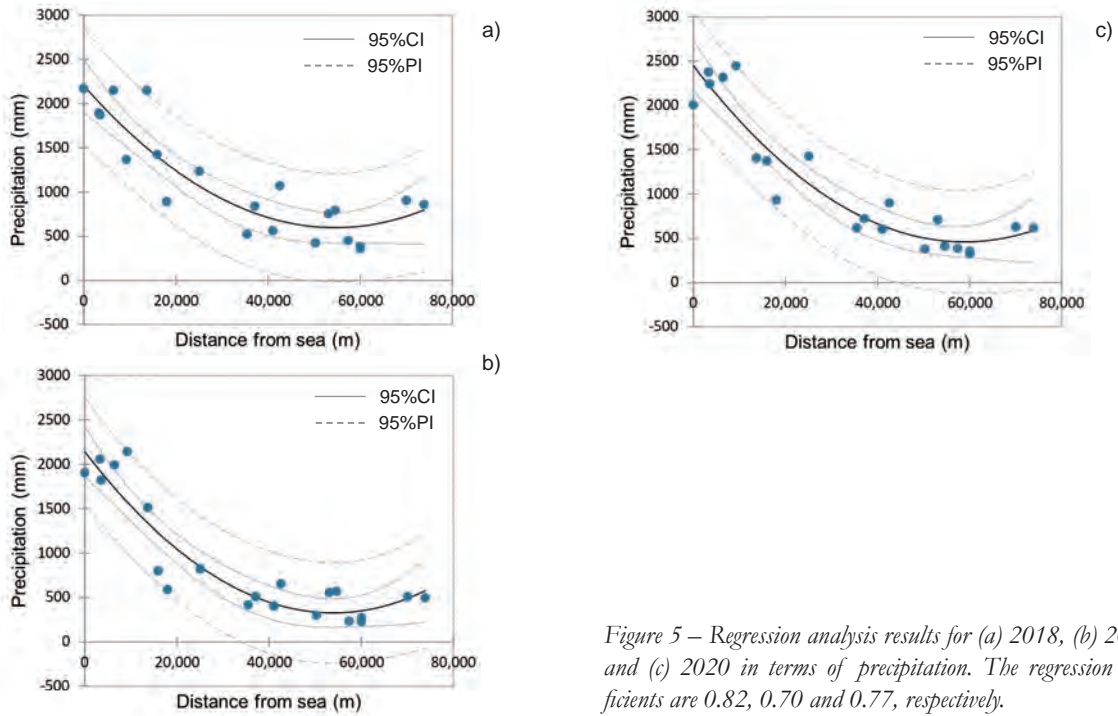


Figure 5 – Regression analysis results for (a) 2018, (b) 2019, and (c) 2020 in terms of precipitation. The regression coefficients are 0.82, 0.70 and 0.77, respectively.

lowing steps were followed in creating interpolated maps for the annual mean temperature and annual total precipitation:

- Formulating prediction models of mean temperature and total precipitation: Regression analysis was used to determine the relationships between: i. the annual mean temperature and altitude; ii. the annual mean temperature and distance from the sea; iii. the annual total precipitation and altitude; and iv. the annual total precipitation and distance from the sea. It was found that there is a linear relationship between the annual mean temperature and elevation (Figure 4), and an exponential relationship between the annual precipitation and distance from the sea (Figure 5). The prediction models obtained from regression formulae are presented in Table 1.
- Generating average temperatures and total precipitation values for virtual stations: 2,500 points

(50×50 squares) were created within the boundaries of the study area using the ArcGIS *Fishnet* tool (Figure 6). The mean temperature and total precipitation values for 2018, 2019 and 2020 were then interpolated for the same points using the ArcGIS *Raster Calculator* tool, using estimation models. Creating 2,500 virtual stations increased the reliability of the interpolated maps for precipitation and temperature by representing as many elevation and distance-from-sea points as possible. The annual mean temperature and total precipitation data were calculated using prediction models for virtual stations.

- Mapping for mean temperature and total precipitation: The interpolated maps for mean temperature and total precipitation for each year were created using the Inverse Distance Weighting method, which has a low root mean square error value; the ArcGIS *Interpolation* tool was used.

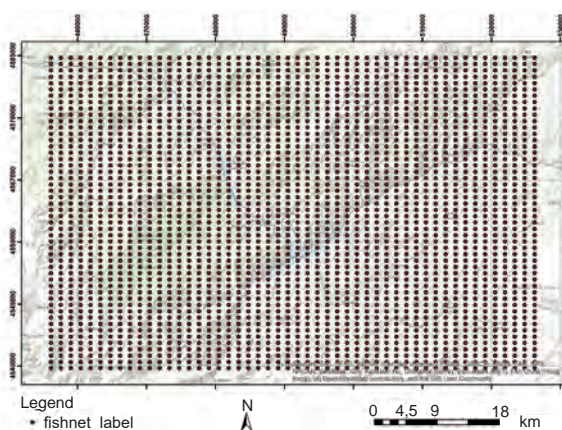


Figure 6 – Distribution of virtual stations in the study area.

Determining the NDVI values of the study area

To calculate the NDVI, band 4 (red) and band 5 (near-infrared) of Landsat 8 OLI/TIRS C2 Level 2 images, with a ground spatial resolution of 30 m, downloaded from United States Geological Survey (USGS) web services (<https://earthexplorer.usgs.gov>) were used (Li et al. 2013). The ArcGIS *Raster calculator* was used for calculations (Eq 1) based on satellite images dated August 2018, August 2019 and August 2020.

$$\text{NDVI} = \frac{(p_{\text{NIR}} - p_{\text{red}})}{(p_{\text{NIR}} + p_{\text{red}})} \quad \text{Eq 1.}$$

NDVI ... Normalized Difference Vegetation Index

p_{NIR} ... Near-infrared band

p_{red} ... Red band

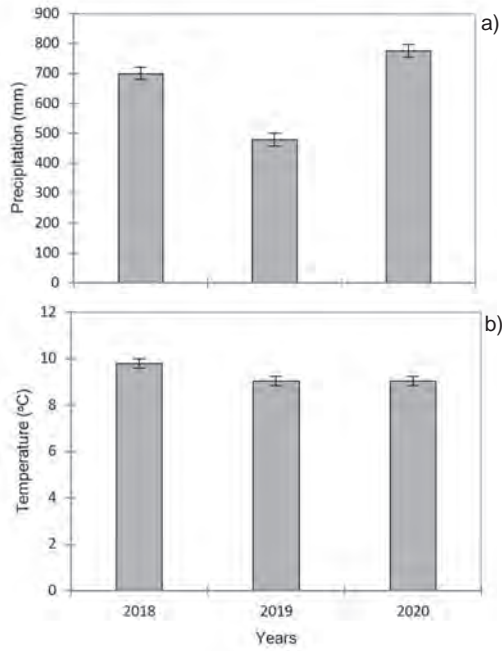


Figure 7 – Variation in (a) annual total precipitation and (b) mean temperature from 2018 to 2020 ($F_{precipitation}$: 483.28; $F_{temperature}$: 48.69; $p < .01$).

Determining relationships between NDVI and abiotic environment

The following steps were followed to determine the variation of NDVI due to the abiotic environment:

- Total annual precipitation, mean annual temperature, elevation, aspect, slope and distance-from-sea layers were converted to vector
- The water surfaces were masked
- NDVI variation was determined from the differences in abiotic environment using ArcGIS *Zonal statistics as table* tools.

Statistical analysis

Analysis of variance (ANOVA) was used to determine the differences among years, elevation and distance from sea in terms of average temperature, total precipitation and NDVI; the Tukey comparison test was used to determine the differences among means. Regression analysis was performed to determine the relationships between the climatic parameters and landforms. XLSTAT software was used for statistical analysis.

Results and Discussion

Spatiotemporal changes in precipitation and temperature

The total precipitation varied in 2018, 2019 and 2020 (Figure 7a). The highest precipitation occurred in 2020, followed by 2018 and 2019. The differences between the years in terms of precipitation were statistically significant. The average temperature also varied significantly over the years. The highest temperature was in 2018, and the lowest in 2020 (Figure 7b).

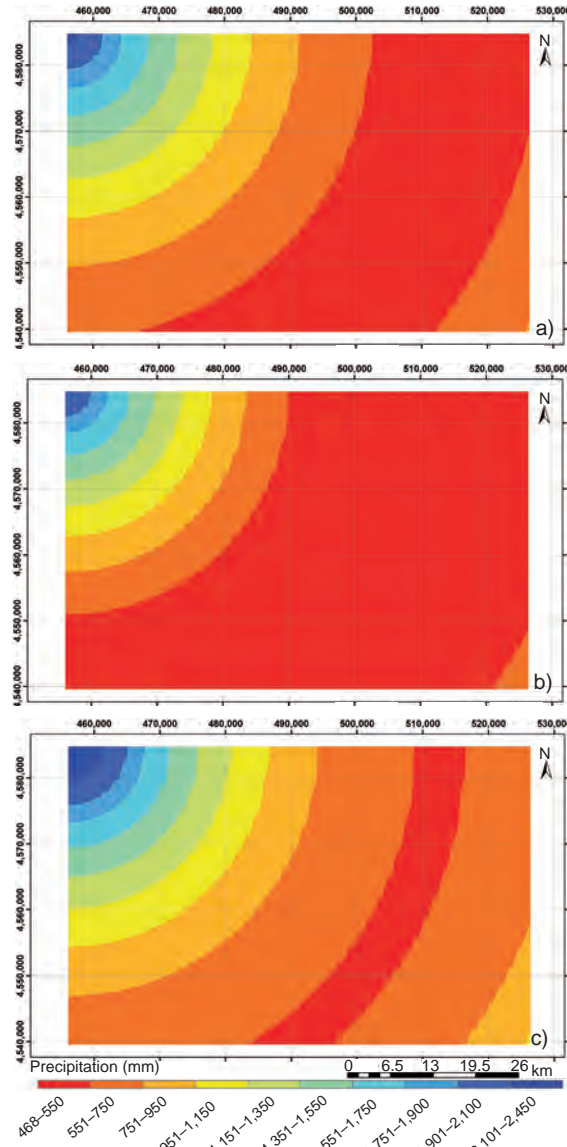


Figure 8 – Spatial variability of precipitation in (a) 2018, (b) 2019, and (c) 2020.

The spatial distributions for annual total precipitation and annual mean temperature are shown in Figures 8 and 9, respectively. The area covered by the lowest precipitation range (< 550 mm) was greater in 2019 than in the other two years. It was the smallest in 2020, which was the most rainy of the three years studied (Figure 8). In line with the results of the variance analysis, the area covered by the highest temperature class (16–17°C) in the distribution map was greater in 2018 than in the other years. It decreased in 2019, and further decreased in 2020 (Figure 9).

The temperature differences among 350 m elevation intervals are statistically significant (Figure 10a). Our results agree with those of previous studies that indicate that mean temperature decreases with increasing elevation (Battey et al. 2019; Poll et al. 2009; Richomme et al. 2010; Yao et al. 2016). The mean temperature also differed significantly depending on the distance from the sea (Figure 10b). However, unlike

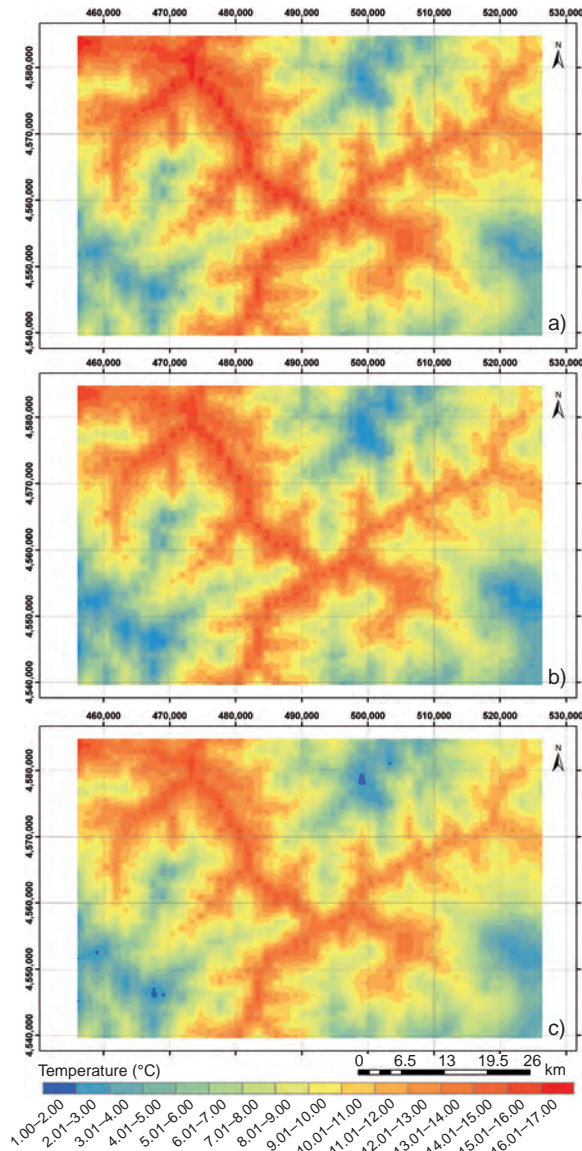


Figure 9 – Spatial variability of temperature in (a) 2018, (b) 2019, and (c) 2020.

the findings for precipitation, the differences did not present a regular trend. They can be explained by the distance from the sea in some parts of the area, but mean temperature was also affected by elevation and aspect, which created higher-temperature microclimates.

The total precipitation differed significantly in relation to elevation (Figure 11a). Researchers have reported a positive linear relationship between elevation and precipitation in arid regions (Yu et al. 2018), while the increase in elevation in humid regions causes a decrease in precipitation (Angelini et al. 2011; Ogino et al. 2016). Further away from the sea, the total annual precipitation changed significantly (Figure 11b). Our findings were consistent with those of other researchers who reported that annual precipitation decreased inland (Bailey 2009; Bao et al. 2021).

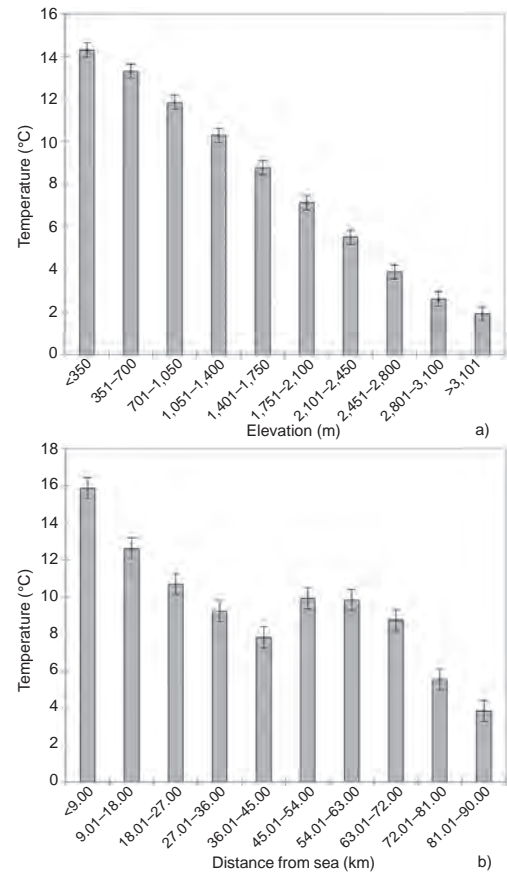


Figure 10 – Variation in average temperature along with (a) elevation and (b) distance from sea ($F_{elevation}^t$: 758.2; $p < .01$; $F_{distance\ from\ sea}^t$: 152.16; $p < .01$).

Spatiotemporal changes to NDVI

The NDVI values varied over the years. The lowest value was achieved in 2019, followed by 2018 and 2020, respectively (Figure 12): vegetative growth and biomass were lowest in 2019, and highest in 2020. It is noteworthy that the highest NDVI (in 2020) coincided with the highest total annual precipitation. The differences between years in terms of the NDVI were statistically significant: it appears that the changes in temperature and precipitation in 2018, 2019 and 2020 caused a difference in NDVI values in these years (a finding reported by other researchers, see Catorci et al. 2021; Zhe & Zhang 2021), and indeed, that the temperature and precipitation changes are one of the main reasons for the differences in NDVI values in the years we studied. The areas highlighted in green in the NDVI distribution map (Figure 13) represent areas with NDVI values above 0.20. Fretwell et al. (2011) reported that areas with an NDVI value of more than 0.20 can be considered vegetated. The differences in the NDVI distribution maps agree with the results of the ANOVA tests, which compared years. In the NDVI distribution map for 2020, the areas above 0.20 were more extensive than in 2019.

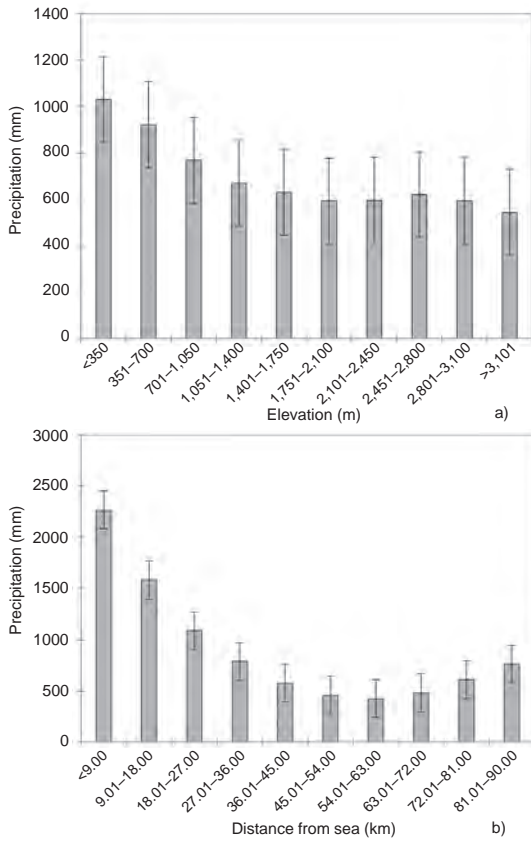


Figure 11 – Variation in average precipitation along with (a) elevation and (b) distance from sea ($F_{elevation} : 3.289; p < .05;$ $F_{distance\ from\ sea} : 44.911; p < .01$).

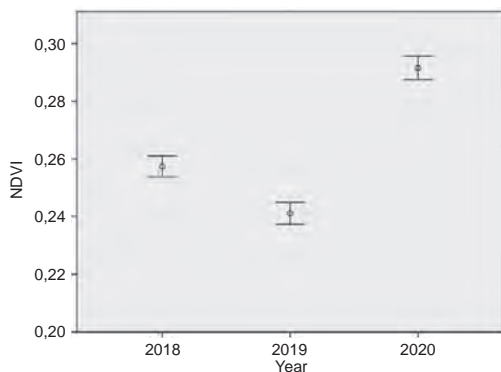


Figure 12 – Variation of the NDVI along with years ($F : 74.74; p < .01$). Error Bars: $\pm 2 SE$

Relationships between NDVI and abiotic environment

Variation in NDVI depending on precipitation and temperature

The NDVI increased significantly with increasing precipitation (Figure 14a). A positive correlation between the amount of precipitation and NDVI has been demonstrated in the literature (Fabricante et al. 2009; Wingate et al. 2019). The NDVI differed significantly in relation to temperature (Figure 14b) and was lowest in the coldest temperature. Although it increased with increasing temperature, the trend above

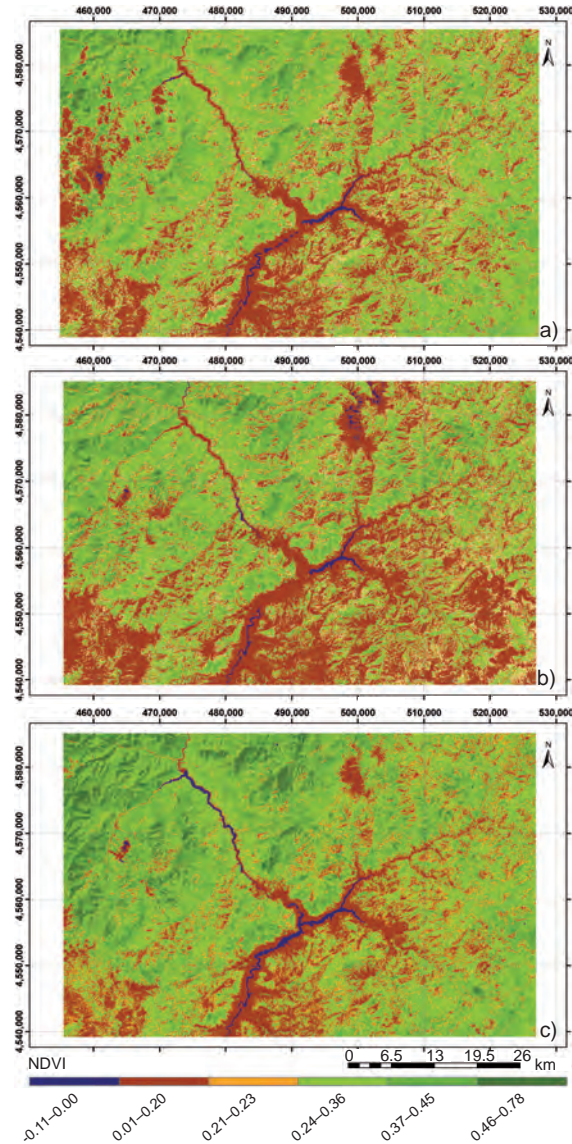


Figure 13 – Spatial variability of NDVI in (a) 2018, (b) 2019, and (c) 2020.

10–11°C was not stable. Low temperatures generally correspond to areas with high elevation, resulting in low vegetation density and, accordingly, low NDVI. The decrease of NDVI at high temperatures may be due to water stress, as researchers have reported that in arid areas the NDVI values decreased as temperature increased (Nse et al. 2020; Rani et al. 2018).

Variation in NDVI depending on elevation

To better interpret the differences in the NDVI caused by the variations in the landforms, both the ANOVA results and the three-year changes in the NDVI are shown in separate graphs. The differences among elevation ranges in terms of NDVI were statistically significant. The lowest NDVI values were found in areas with an altitude above 3,100 m, the highest at 1,050–1,400 m (Figure 15a). The most important information in Figure 15b is that unlike in 2018 and 2020, the altitude range where NDVI started to de-

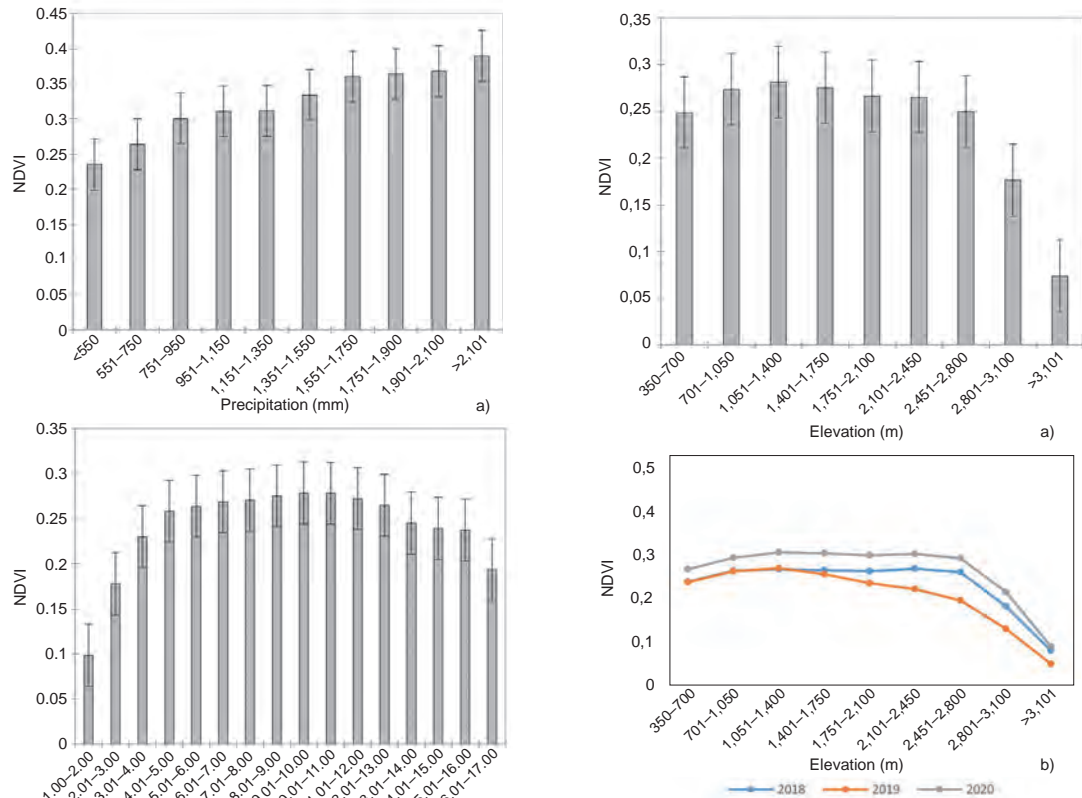


Figure 14 – Variations in average NDVI along with (a) precipitation and (b) temperature ($F_{precipitation}$: 8.042; $p < .01$; $F_{temperature}$: 8.062; $p < .01$).

crease in 2019 (the driest year) was 1,050–1,400 m. The fact that NDVI values decrease faster in alpine zones during arid periods means that the plants growing in such areas are more affected by dry periods. Researchers have stated that warmer temperatures and changing precipitation patterns due to climate change will increase the relative importance of soil and atmospheric droughts in limiting productivity across different ecosystems, especially fragile ones that are extremely sensitive to environmental changes (Tello-García et al. 2020; Xu et al. 2021). In line with our findings, it has been reported that an increase in temperature decreases the productivity of alpine pastures (Tello-García et al. 2020; Xu et al. 2021).

Variation in NDVI depending on the distance from the sea

The NDVI differed significantly in relation to distance from the sea (Figure 16a). NDVI values were highest on the coastal side of the study area, decreasing with increased distance from the sea, falling to their lowest around 45–54 km inland (the mid-point for distance from the coast), and increasing again from this point. In areas that are more than 45 km from the coast and where precipitation is below 500 mm, the limited increase in precipitation (up to 632 mm) in 2019 did not increase the NDVI. However, an upward trend was observed in these areas in the rainier years

Figure 15 – (a) Variations in average NDVI along with elevation ($F_{elevation}$: 13.818; $p < .01$); (b) change in NDVI in terms of elevation over time.

of 2018 and 2020 (Figure 16b). The change in NDVI by distance from the sea may be due to variations in precipitation and temperature. Precipitation greatly impacts the amount of vegetation present in any given year (Wingate et al. 2019).

Variation in NDVI depending on aspect

Differences in aspect caused significant changes in the NDVI (Figure 17a). In all three years, the highest NDVI value was in the east, and the lowest in the northwest (Figure 17b). Topographical aspect modifies the amount of solar radiation received by a surface (Geiger, 1965; Oke, 1987; Bennie et al. 2008). In humid regions, vegetation is denser on the east and west sides because of the greater insolation; higher NDVI values were therefore expected on the east-facing slopes of the study area. In agreement with our results, previous studies also reported that vegetation is denser in east- and west-facing areas in humid regions (Jin et al. 2008; Zhan et al. 2012).

Variation in NDVI depending on slope

The change in NDVI depending on the slope was statistically significant (Figure 18a). The study area is predominantly mountainous, and urban areas and agricultural fields are concentrated in regions with gentle slopes. Thus, the NDVI values were the lowest in areas with a slope of 0–0.5%. These increased with increased slope, but then showed a decreasing trend be-

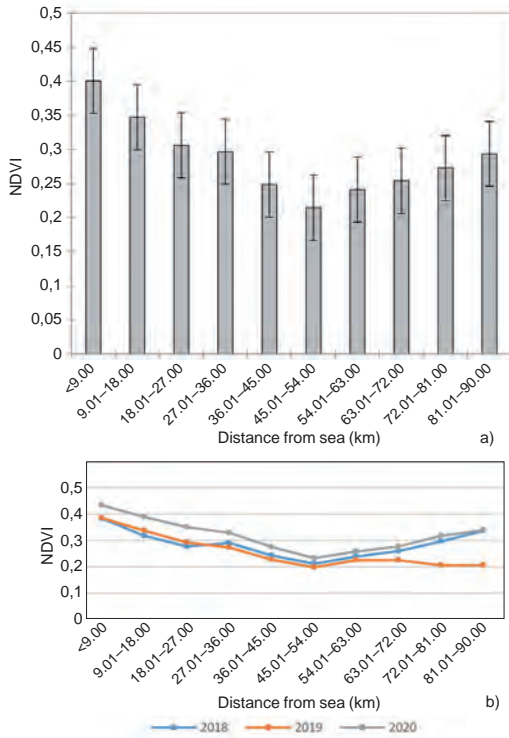


Figure 16 – (a) Variations in average NDVI along with distance from the sea ($F_{distance\ from\ sea}: 5.757; p < .01$); (b) change in NDVI in terms of distance from the sea over time.

tween the ranges of 30–45% and > 45% (Figure 18b). The main reason for this is that human activities such as urbanization, tree-felling and agricultural activity are rare on steep terrain. The low NDVI in the steep parts of the study area may be due to shallow soil, low water availability for plants because of very high runoff, and high surface temperatures in sunny aspects. Consistent with our findings, Xiong et al. (2021) reported that the NDVI decreased in areas with a steep gradient.

Conclusion

The NDVI used for qualitative and quantitative estimation of vegetation dynamics is influenced by precipitation, temperature, elevation, distance from sea, aspect and slope. Landform data can be determined from satellite images using geographic information systems. Based on landform data and using regression analysis, patterns in climate dynamics can be predicted. The results showed that in our particular study area located in Artvin: (i) temperature can be predicted by elevation, and precipitation by distance from the sea; (ii) changes in annual mean temperature and annual total precipitation alter the NDVI; (iii) NDVI varies depending on the landform; (iv) the vegetation of alpine zones is more sensitive to dry periods.

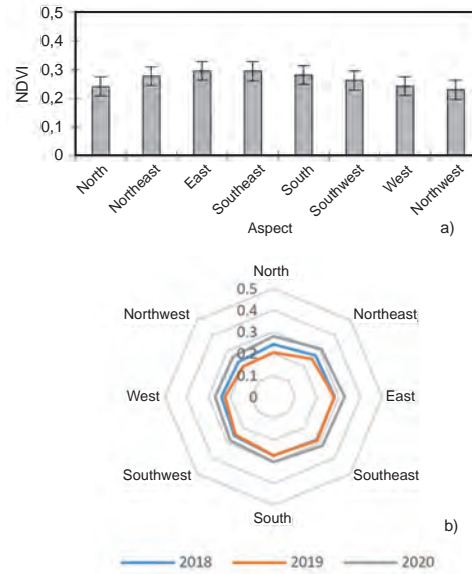


Figure 17 – (a) Variations in NDVI along with aspect ($F_{aspect}: 2.679; p < .05$); (b) change in NDVI in terms of aspect over time.

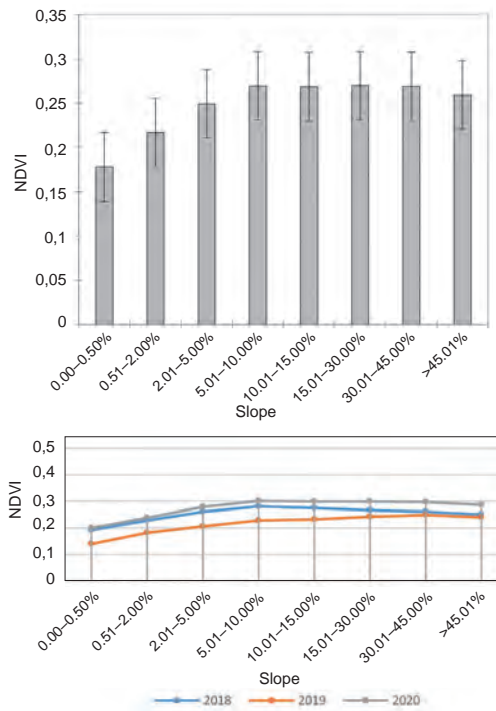


Figure 18 – (a) Variations in NDVI along with slope ($F_{slope}: 3.373; p < .05$); (b) change in NDVI in terms of slope over time.

References

- Angelini, I. M. Garstang, R. E. Davis, B. Hayden, D.R. Fitzjarrald, D.R. Legates, S. Greco, S. Macko & V. Connors 2011. On the coupling between vegetation and the atmosphere. *Theoretical and Applied Climatology* 105(1): 243–261. Doi: 10.1007/s00704-010-0377-5
- ASF DAAC 2015. ALOS PALSAR_Radiometric_Terrain_Corrected_low_res; Includes Material © JAXA/METI 2007. Accessed through ASF DAAC 07.10.2021. Doi: 10.5067/JBYK3J6HFSVF
- Bailey, R.G. 2009. Ecosystem Geography: From Ecoregions to Sites. Available at: <https://books.google.com.tr/books?id=9wC0Dd5EsJYC>
- Bao, Z., J. Zhang, G. Wang, T. Guan, J. Jin, Y. Liu, M. Li & T. Ma 2021. The sensitivity of vegetation cover to climate change in multiple climatic zones using machine learning algorithms. *Ecological Indicators* 124: 107443. Doi: 10.1016/j.ecolind.2021.107443
- Batthey, C.J., L.M. Otero, G.C. Gorman, P.E. Hertz, B.C. Lister, A. García, P.A. Burrowes & R.B. Huey 2019. Why Montane Anolis Lizards are Moving Downhill While Puerto Rico Warms. *BioRxiv* 751941. Doi: 10.1101/751941
- Bennie, J., B. Huntley, A. Wiltshire, M.O. Hill & R. Baxter 2008. Slope, aspect and climate: Spatially explicit and implicit models of topographic microclimate in chalk grassland. *Ecological Modelling* 1: 47–59.
- Catorci, A., R. Lulli, L. Malatesta, M. Tavoloni & F.M. Tardella 2021. How the interplay between management and interannual climatic variability influences the NDVI variation in a sub-Mediterranean pastoral system: Insight into sustainable grassland use under climate change. *Agriculture, Ecosystems & Environment* 314: 107372. Doi: 10.1016/j.agee.2021.107372
- Choubin, B., F. Soleimani, A. Pirnia, F. Sajedi-Hosseini, H. Alilou, O. Rahmati, A.M. Melesse, V.P. Singh & H. Shahab 2019. Effects of drought on vegetative cover changes: Investigating spatiotemporal patterns. *Extreme Hydrology and Climate Variability*: 213–222. Doi: 10.1016/B978-0-12-815998-9.00017-8
- Chu, H.S., S. Venevsky, C. Wu & M.H. Wang 2019. NDVI-based vegetation dynamics and its response to climate changes at Amur-Heilongjiang River Basin from 1982 to 2015. *Science Total Environment* 650: 2051–2062. Doi: 10.1016/j.scitotenv.2018.09.115
- El-Keblawy, A., M.A. Abdelfattah & A. Khedr 2015. Relationships between landforms, soil characteristics and dominant xerophytes in the hyper-arid northern United Arab Emirates. *Journal of Arid Environments* 117: 28–36. Doi: 10.1016/j.jaridenv.2015.02.008
- Eminağaoğlu, Ö., H. Akyıldırım Beğen & G. Aksu 2015. Artvin'in doğal bitkileri. Promat Basım Yayım. Doi: 10.13140/RG.2.1.4312.3608
- Fabricante, I., M. Oesterheld & J.M. Paruelo. 2009. Annual and seasonal variation of NDVI explained by current and previous precipitation across Northern Patagonia. *Journal of Arid Environments* 73(8): 745–753. Doi: 10.1016/j.jaridenv.2009.02.006
- FAO 2021. *FAO Soils Portal. Global Terrain Slope and Aspect Data*. Available at: <http://www.fao.org/soils-portal/data-hub/soil-maps-and-databases/harmonized-world-soil-database-v12/terrain-data/en/> (accessed: 25/09/2021)
- Flores, D., E. Ocaña & A.I. Rodríguez 2019. Relationships between landform properties and vegetation patterns in the Cerro Zonda Mt., Central Precordillera of San Juan. Argentina. *Journal of South American Earth Sciences* 96: 102359. Doi: 10.1016/j.jsames.2019.102359
- Fretwell, P.T., P. Convey, A.H. Fleming, H.J. Peat & K.A. Hugles 2011. Detecting and mapping vegetation distribution on the Antarctic Peninsula from remote sensing data. *Polar Biology* 34: 273–281.
- Gao, J.G., Y.L. Zhang, L.S. Liu & Z.F. Wang 2014. Climate change as the major driver of alpine grasslands expansion and contraction: A case study in the Mt. Qomolangma (Everest) National Nature Preserve, southern Tibetan, Plateau. *Quaternary International* 336: 108–116.
- Geiger, R. 1965. *The Climate Near the Ground*. Cambridge, MA.
- Ghebregabher, M.G., T. Yang, X. Yang & T. Eyasu Serek 2020. Assessment of NDVI variations in responses to climate change in the Horn of Africa. *The Egyptian Journal of Remote Sensing and Space Science* 23(3): 249–261. Doi: 10.1016/j.ejrs.2020.08.003
- Hou, W., J. Gao, S. Wu & E. Dai 2015. Interannual variations in growing-season NDVI and its correlation with climate variables in the southwestern karst region of China. *Remote Sensing* 7: 11105–11124.
- Jiang, S., X. Chen, K. Smettem & T. Wang 2021. Climate and land use influences on changing spatiotemporal patterns of mountain vegetation cover in southwest China. *Ecological Indicators* 121: 107193. Doi: 10.1016/j.ecolind.2020.107193
- Jin, X.M., Y.K. Zhang, M.E. Schaepman, J.G.P.W. Clevers, Z. Su, J. Clevers & M. Schaepman 2008. *Impact of elevation and aspect on the spatial distribution of vegetation in the Gilian mountain area with remote sensing data*. Available at: <http://heihe.westgis.ac.cn> (accessed: 07/07/2021)
- Kimmins, J.P. 2004. *Forest Ecology: A Foundation for Sustainable Forest Management and Environmental Ethics in Forestry*. Prentice Hall. Available at: <https://books.google.com.tr/books?id=0LEsAQAAMAAJ>
- Li, P., L. Jiang & Z. Feng 2013. Cross-comparison of vegetation indices derived from landsat-7 enhanced thematic mapper plus (ETM+) and landsat-8 operational land imager (OLI) sensors. *Remote Sensing* 6(1): 310–329.
- Li, P., J. Wang, M. Liu, Z. Xue, A. Bagherzadeh & M. Liu. 2021. Spatio-temporal variation characteristics of NDVI and its response to climate on the Loess Plateau from 1985 to 2015. *CATENA* 203: 105331. Doi: 10.1016/j.catena.2021.105331
- Li, Q., X. Shi, & Q. Wu. 2020. Exploring suitable topographical factor conditions for vegetation growth in Wanhuigou catchment on the Loess Plateau, Chi-

- na: A new perspective for ecological protection and restoration. *Ecological Engineering* 158: 106053. Doi: 10.1016/j.ecoleng.2020.106053
- Liu, H., M. Zhang, Z. Lin & X. Xu. 2018. Spatial heterogeneity of the relationship between vegetation dynamics and climate change and their driving forces at multiple time scales in Southwest China. *Agricultural and Forest Meteorology* 256: 10–21.
- Liu, L., Y. Wang, Z. Wang, D. Li, Y. Zhang, D. Qin & S. Li 2019. Elevation-dependent decline in vegetation greening rate driven by increasing dryness based on three satellite NDVI datasets on the Tibetan Plateau. *Ecological Indicators* 107: 105569. Doi: 10.1016/j.ecolind.2019.105569
- Mokarram, M. & D. Sathyamoorthy 2015. Modeling the relationship between elevation, aspect and spatial distribution of vegetation in the Darab Mountain, Iran using remote sensing data. *Modeling Earth Systems and Environment* 1(4): 1–6. Doi: 10.1007/s40808-015-0038-x
- Myneni, R.B. & D.L. Williams 1994. On the relationship between FAPAR and NDVI. *Remote Sensing of Environment* 49: 200–211. Doi: 10.1016/0034-4257(94)90016-7
- Nanzad, L., J. Zhang, B. Tuvdendorj, M. Nabil, S. Zhang & Y. Bai 2019. NDVI anomaly for drought monitoring and its correlation with climate factors over Mongolia from 2000 to 2016. *Journal of Arid Environments* 164: 69–77. Doi: 10.1016/j.jaridenv.2019.01.019
- Nemani, R.R., C.D. Keeling, H. Hashimoto, W.M. Jolly, S.C. Piper, C.J. Tucker, R.B. Myenni & S.W. Running 2003. Climate-driven increases in global terrestrial net primary production from 1982 to 1999. *Science* 300(5625): 1560–1563.
- Nse, O.U., C.J. Okolie & V.O. Nse 2020. Dynamics of land cover, land surface temperature and NDVI in Uyo City, Nigeria. *Scientific African* 10: e00599. Doi: 10.1016/j.sciaf.2020.e00599
- Ogino, S.-Y., M.D. Yamanaka, S. Mori & J. Matsumoto 2016. How Much is the Precipitation Amount over the Tropical Coastal Region? *Journal of Climate* 29(3): 1231–1236. Doi: 10.1175/JCLI-D-15-0484.1
- Oke, T.R. 1987. *Boundary Layer Climates* (2nd ed.). London
- Pang, G., X. Wang & M. Yang 2017. Using the NDVI to identify variations in, and responses of, vegetation to climate change on the Tibetan Plateau from 1982 to 2012. *Quaternary International* 444: 87–96.
- Panigrahi, S., K. Verma & P. Tripathi 2021. Review of MODIS EVI and NDVI data for data mining applications. In: Thwel, T.T. & G.R. Sinha (eds.), *Data Deduplication Approaches*: 231–253. Doi: 10.1016/b978-0-12-823395-5.00018-5
- Peilin, L., D. Zhu, Y. Wang & D. Liu 2020. Elevation dependence of drought legacy effects on vegetation greenness over the Tibetan Plateau. *Agricultural and Forest Meteorology* 295: 108190. Doi: 10.1016/j.agrformet.2020.108190
- Piao, S., A. Mohammat, J. Fang, Q. Cai & J. Feng 2006. NDVI-based increase in growth of temperate grasslands and its responses to climate changes in China. *Global Environmental Change* 16(4): 340–348. Doi: 10.1016/j.gloenvcha.2006.02.002
- Poll, M., B.J. Naylor, J.M. Alexander, P.J. Edwards & H. Dietz 2009. Seedling establishment of Asteraceae forbs along altitudinal gradients: a comparison of transplant experiments in the native and introduced ranges. *Diversity and Distributions* 15(2): 254–265. Doi: 10.1111/j.1472-4642.2008.00540.x
- Rani, M., P. Kumar, P.C. Pandey, P.K. Srivastava, B.S. Chaudhary, V. Tomar & V.P. Mandal 2018. Multi-temporal NDVI and surface temperature analysis for Urban Heat Island inbuilt surrounding of sub-humid region: A case study of two geographical regions. *Remote Sensing Applications: Society and Environment* 10: 163–172. Doi: 10.1016/j.rsase.2018.03.007
- Richomme, C., E. Afonso, V. Tolon, C. Ducrot, L. Halos, A. Alliot, C. Perret, M. Thomas, P. Boireau & E. Gilot-Fromont 2010. Seroprevalence and factors associated with *Toxoplasma gondii* infection in wild boar (*Sus scrofa*) in a Mediterranean island. *Epidemiology and Infection* 138(9): 1257–1266. Doi: 10.1017/S0950268810000117
- Sanz, E., A. Saa-Requejo, C.H. Díaz-Ambrona, M. Ruiz-Ramos, A.E. Rodríguez-Iglesias, P. Esteve, B. Soriano & A.M. Tarquis 2021. Normalized Difference Vegetation Index Temporal Responses to Temperature and Precipitation in Arid Rangelands. *Remote Sensing* 13, 840. Doi: 10.3390/rs13050840.
- Tello-García, E., L. Huber, G. Leitinger, A. Peters, C. Newesely, M.-E. Ringler & E. Tasser 2020. Drought- and heat-induced shifts in vegetation composition impact biomass production and water use of alpine grasslands. *Environmental and Experimental Botany* 169: 103921. Doi: 10.1016/j.envexpbot.2019.103921
- Wingate, V.R., S.R. Phinn & N. Kuhn 2019. Mapping precipitation-corrected NDVI trends across Namibia. *Science of the Total Environment* 684: 96–112. Doi: 10.1016/j.scitotenv.2019.05.158
- Wu, D., X. Zhao, S. Liang, T. Zhou, K. Huang, B. Tang & W. Zhao 2015. Time-lag effects of global vegetation responses to climate change. *Global Change Biology* 21(9): 3520–3531. Doi: 10.1111/gcb.12945
- Wu, Y., W. Li, Q. Wang & S. Yan 2016. Landslide susceptibility assessment using frequency ratio, statistical index and certainty factor models for the Gangu County, China. *Arabian Journal of Geosciences* 9 (2). Doi: 10.1007/s12517-015-2112-0
- Xiong, Y., Y. Li, S. Xiong, G. Wu & O. Deng 2021. Multi-scale spatial correlation between vegetation index and terrain attributes in a small watershed of the upper Minjiang River. *Ecological Indicators* 126: 107610. Doi: 10.1016/j.ecolind.2021.107610
- Xu, H.J., X.P. Wang & T.B. Yang 2017. Trend shifts in satellite-derived vegetation growth in Central Eurasia, 1982–2013. *Science of the Total Environment* 579: 1658–1674. Doi: 10.1016/j.scitotenv.2016.11.182.

Xu, M., T. Zhang, Y. Zhang, N. Chen, J. Zhu, Y. He, T. Zhao & G. Yu 2021. Drought limits alpine meadow productivity in northern Tibet. *Agricultural and Forest Meteorology* 303: 108371. Doi: 10.1016/j.agrformet.2021.108371

Yang, J., A. El-Kassaby & W. Guan 2020. The effect of slope aspect on vegetation attributes in a mountainous dry valley, Southwest China. *Science report* 10: 16465. Doi: 10.1038/s41598-020-73496-0

Yao, J., Q. Yang, W. Mao, Y. Zhao & X. Xu 2016. Precipitation trend – Elevation relationship in arid regions of China. *Global and Planetary Change* 143: 1–9. Doi: 10.1016/j.gloplacha.2016.05.007

Yu, H., L. Wang, R. Yang, M. Yang & R. Gao 2018. Temporal and spatial variation of precipitation in the Hengduan Mountains region in China and its relationship with elevation and latitude. *Atmospheric Research* 213: 1–16. Doi: 10.1016/j.atmosres.2018.05.025

Zhan, Z.-Z., H.-B. Liu, H.-M. Li, W. Wu & B. Zhong 2012. The Relationship between NDVI and Terrain Factors. A Case Study of Chongqing. *Procedia Environmental Sciences* 12: 765–771. Doi: 10.1016/j.proenv.2012.01.347

Zhang, B., J. Cao, Y. Bai, X. Zhou, Z. Ning, S. Yang & L. Hu 2013. Effects of rainfall amount and frequency on vegetation growth in a Tibetan alpine meadow. *Climatic Change* 118: 197–212

Zhe, M. & X. Zhang 2021. Time-lag effects of NDVI responses to climate change in the Yamzhog

Yumco Basin, South Tibet. *Ecological Indicators* 124: 107431. Doi: 10.1016/j.ecolind.2021.107431

Zhu, Z., Y. Fu, C.E. Woodcock, P. Olofsson, C.E. Vogelmann, C. Holden, M. Wang, S. Dai & Y. Yu 2016. Including land cover change in analysis of greenness trends using all available Landsat 5, 7, and 8 images: A case study from Guangzhou, China (2000–2014). *Remote Sensing of Environment* 185: 243–257.

Authors

Hilal Turgut

is an Associate Professor at Karadeniz Technical University, Department of Landscape Architecture. Her main interests are landscape planning, ecosystem services, protected areas and geographic information systems. Karadeniz Technical University Faculty of Forestry, Landscape Architecture Department, 61080 Trabzon, Turkey.

Bülent Turgut

is an Associate Professor at Karadeniz Technical University, Department of Soil and Ecology. His main interests are soil degradation, ecosystem services and geographic information systems. Karadeniz Technical University Faculty of Forestry, Soil and Ecology Department, 61080 Trabzon, Turkey.